Contribution to the Study, Design and Production of a Miniaturized Adjustable Phase Coupler for Beam Steering Applications

Asmae Mimouni[1], [*], Moustapha El Bakkali[2], and Naima Amar Touhami[2]

Abstract—In this article, we present the design and production of a miniaturized adjustable coupler with optimized dimensions of 48 mm in length and 31 mm in width. This coupler offers the possibility of covering all phases [0, 45°, 90°, 120°, and 180°]. To be able to achieve this, the proposed coupler can be adjusted through the implementation of six SMV2019-079LF diodes which allow shifting from one phase to another. This new flexibility, in terms of phase shifting, can greatly improve the multifunctional use of this small and efficient coupler, in particular, in comparison with previously improved phase shifting couplers which are limited to one or two phases. The high performance and efficiency have been verified by the results obtained by simulation and measurement.

1. INTRODUCTION

Adjustable phase couplers are in rising demand for a variety of modern systems, such as communication systems, microwave, and millimetre wave's applications. In the last decade, many studies have been brought upon this subject [1, 2]. Nevertheless, adjustable miniaturized couplers are still understudied even with the increasing use of phase-shifter couplers, thus, this paper proposes a contribution to the study of performances of an adjustable coupler with low weight, low cost, and high integrity.

The previous studies dealing with the output shift of phase were mostly focused on the difference of either 90° or 180° to realize a typical 4 × 4 butler matrix by using a microstrip line or adopting different arrangements for couplers [3, 4]. Other studies opted for a 45° phase shifting by using a substrate integrated waveguide broadband self-compensating phase shifter, and in this case, phase shifts were obtained by two different structures, namely, delay line and equal-length unequal-width phase shifter [5], while in [6], a filtering coupled-line trans-directional (CL-TRD) coupler with broadband bandpass response was proposed. In the same line, Muquaddar et al. [7] presented a novel branch-line coupler with improved bandwidth and reduced size, and in [8] a design of Full-360° Reflection-Type Phase Shifter was achieved using Trans-Directional Coupler with Multi-Resonance Loads.

In this paper, we extend the ranges of phases to cover the most relevant used phases in any possible application, mainly 0, 45°, 90°, 120°, and 180°. This can be achieved by introducing six varactor diodes to the traditional directional coupler to adjust it to the desired phase without compromising any of its given characteristics. The adjustable coupler will be used in a Butler matrix. A Butler matrix is a very advantageous beam-forming network due to its ability to form orthogonal beams in a simple design and is commonly found in microwave circuits.

[*] Corresponding author: Asmae Mimouni (amalmimouni@imamu.edu.sa).

[1] Department of Physics, College of Science, Imam Mohammad Ibn Saud Islamic University (IMSIU), P. O. Box 90950, Riyadh 11623, Saudi Arabia. [2] Information System and Telecommunication Laboratory, Faculty of Science, Abdelmalek Essaadi University, BP. 2121, M'Hannech II, Tetuan 93030, Morocco.

2. THEORY AND DESIGN

A coupler is a four-port microwave device, and it can be categorized by its main parameters, such as the bandwidth, insertion loss, phase shift between ports, loss, coupling ratio, and isolation. It is also defined as a lossless passive component on isotropic support [9]. Figure 1 shows the geometry of a directional coupler, and each of the coupler ports is adapted; the power injected into an input port (P_1) is divided between the two output ports (P_3 and P_4), and no power is coupled to port P_4.

Each coupler is characterized by its S matrix that can be found using S-parameter analysis. Via a meticulous analysis, we can find that the S-matrix is given as follows [10]:

$$S = \frac{-1}{\sqrt{2}} \begin{bmatrix} 0 & j & 1 & 0 \\ j & 0 & 0 & 1 \\ 1 & 0 & 0 & j \\ 0 & 1 & j & 0 \end{bmatrix} \tag{1}$$

These S-parameters represent incident and reflected voltage waves at the different ports in a microwave network and will be thoroughly examined in this work.
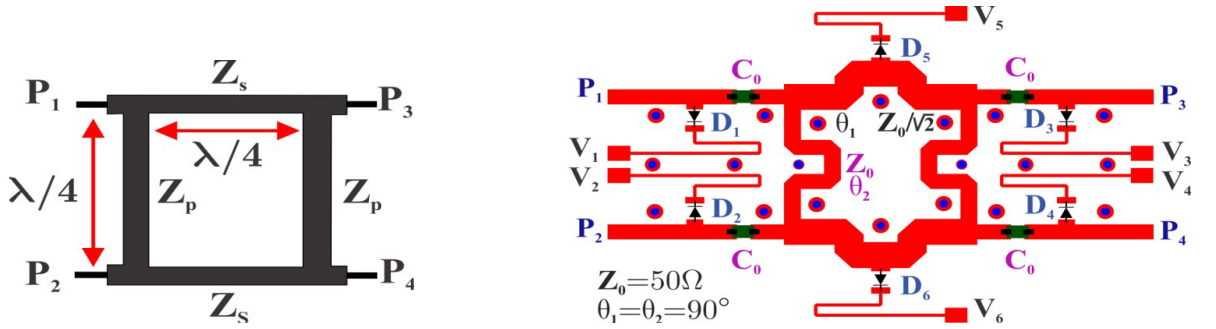

Figure 1. Typical geometry of a directional coupler.

Figure 2. The layout of the proposed phase adjustable coupler.

The proposed phase adjustable coupler (Fig. 2) is a directional coupler designed on an FR4 substrate. The miniaturized phase adjustable coupler has been made with the optimized dimensions of 48 mm in length and 31 mm in width, and the vias are used for coupling between the $\lambda/4$ bias lines (meander lines). This coupler is designed to operate at the central frequency of 2.4 GHz.

The six varactor diodes are added to shift the phase of ports P3 and P4. Their positions and number are optimized to cover the range of phases from $0°$ to $180°$. The type of diode chosen in this work is a commercial diode SMV2019-079LF, with a reverse voltage of 22 V, a forward current of 20 mA, and a power dissipation of 250 mW. The capacitors C are connection capacitors used to block the passage of the DC component between the diodes.

Figure 3 shows the proposed adjustable coupler scheme. The diodes are modeled by 2C capacitors. XX' and YY' are planes of symmetry used to facilitate the analysis of the schematic with the even and odd method. The input impedances of each mode of the sub-circuits in Figures 3(b), (c), (d), and (e) are:

$$Z_{eo} = \frac{1}{\dfrac{j\tan(\theta_2)}{Z_2} + 2jc\omega + \dfrac{1}{jZ_1\tan(\theta_1)}} = \frac{1}{x} \tag{2}$$

$$Z_{oe} = \frac{1}{\dfrac{j\tan(\theta_2)}{Z_2} + 2jc\omega + \left(\dfrac{Z_1}{j\tan(\theta_1)} + \dfrac{1}{jc\omega}\right)} = \frac{1}{z} \tag{3}$$

$$Z_{oo} = \frac{1}{\dfrac{1}{jZ_2\tan(\theta_2)} + 2jc\omega + \dfrac{1}{jZ_1\tan(\theta_1)}} = \frac{1}{y} \tag{4}$$
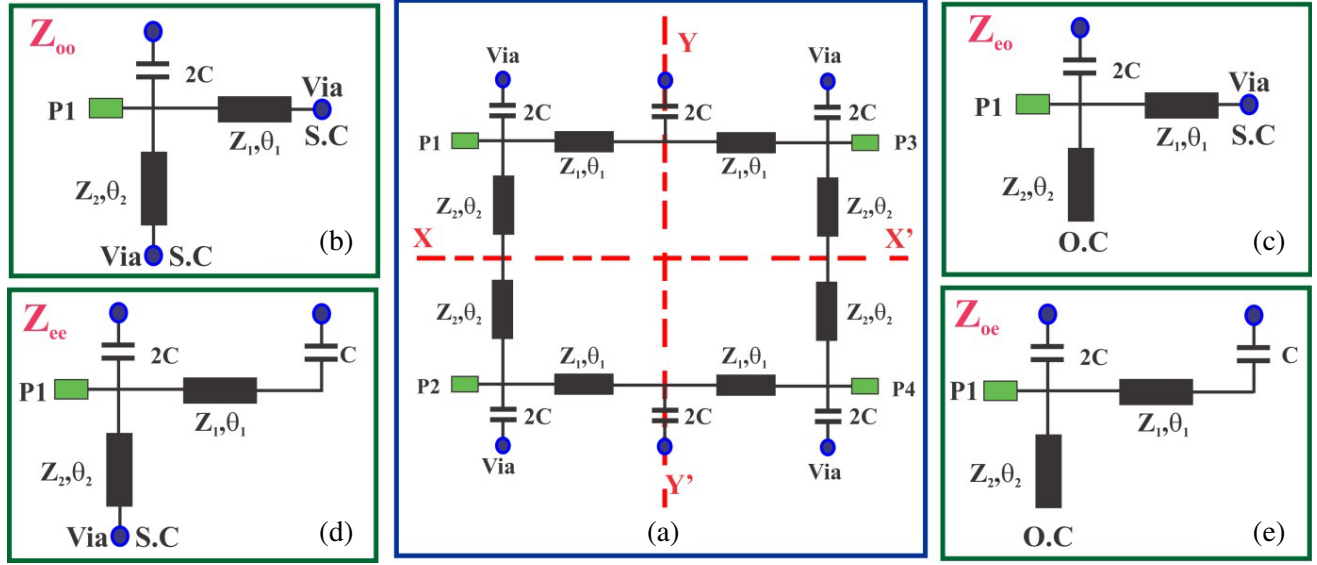
Figure 3. (a) Even-odd mode of proposed adjustable coupler for different excitation: (b) odd-odd mode, (c) even-odd mode, (d) even-even mode and (e) odd-even mode.

$$Z_{ee} = \frac{1}{\dfrac{1}{jZ_2 \tan(\theta_2)} + 2jc\omega + \left(\dfrac{Z_1}{j\tan(\theta_1)} + \dfrac{1}{jc\omega}\right)} = \frac{1}{m} \tag{5}$$

The reflection coefficients corresponding to each mode are:

$$\Gamma_{ee} = \frac{Z_{ee} - Z_0}{Z_{ee} + Z_0} = \frac{1/m - Z_0}{1/m + Z_0} \tag{6}$$

$$\Gamma_{eo} = \frac{Z_{eo} - Z_0}{Z_{eo} + Z_0} = \frac{1/x - Z_0}{1/x + Z_0} \tag{7}$$

$$\Gamma_{oo} = \frac{Z_{oo} - Z_0}{Z_{oo} + Z_0} = \frac{1/y - Z_0}{1/y + Z_0} \tag{8}$$

$$\Gamma_{oe} = \frac{Z_{oe} - Z_0}{Z_{oe} + Z_0} = \frac{1/z - Z_0}{1/z + Z_0} \tag{9}$$

The S-parameters as a function of the reflection coefficients of each mode can be calculated using the following expressions:

$$S_{11} = \frac{(\Gamma_{ee} + \Gamma_{oe}) + (\Gamma_{eo} + \Gamma_{oo})}{4} \tag{10}$$

$$S_{21} = \frac{(\Gamma_{ee} + \Gamma_{oe}) - (\Gamma_{eo} + \Gamma_{oo})}{4} \tag{11}$$

$$S_{31} = \frac{(\Gamma_{ee} - \Gamma_{oe}) + (\Gamma_{eo} - \Gamma_{oo})}{4} \tag{12}$$

$$S_{41} = \frac{(\Gamma_{ee} - \Gamma_{oe}) - (\Gamma_{eo} - \Gamma_{oo})}{4} \tag{13}$$

where $\theta_1 = \theta_2 = 45°$; $Z_1 = 35.35\,\Omega$; $Z_2 = Z_0 = 50\,\Omega$ and $\omega = 2\pi f$.

3. SIMULATION RESULTS

In order to verify the feasibility of the adjustable coupler proposed in the present study, the simulated results were obtained with electromagnetic simulation and co-simulation using the Advanced Design
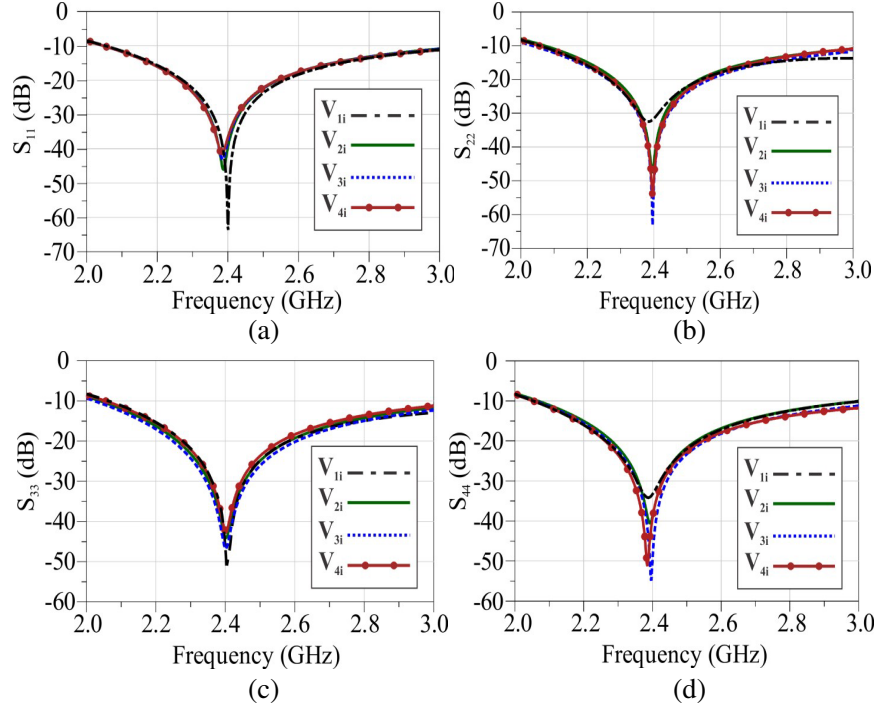
Figure 4. Simulation results of the reflection coefficient at: (a) port P_1, (b) port P_2, (c) port P_3 and (d) port P_4.
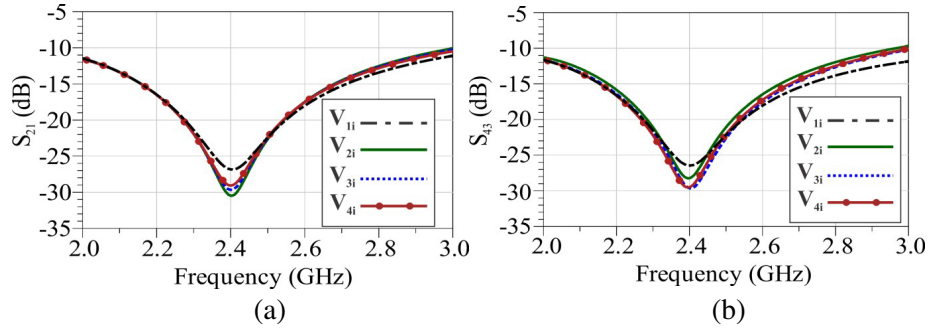

Figure 5. Simulation results of the isolations coefficients at: (a) S_{21} between P_1 and P_2, (b) S_{43} between P_3 and P_4.

System (ADS) software of the Keysight Technologies PathWave Design [11].

As indicated before, the performances of a coupler device are determined by the elements of its correspondent S matrix. Firstly, we examine the return reflection coefficient. As shown in Figure 4, the coefficient of reflection S_{ii} for each port is in the vicinity of -40 dB around the frequency 2,4 GHz which indicates that there is total power transmission in this coupler.

The same remark can be made for the isolation coefficient between port 1 and port 2, and between port 3 and port 4.

Figure 5 shows clearly that there is a perfect isolation between the ports P_1 and P_2, and the ports P_3 and P_4 since the values of S_{21} and S_{43} reach -30 dB at the working frequency of the present studied coupler.

It is also important to note that the co-simulation results show that the amplitudes of the S-parameters of the studied coupler are slightly dependent on the variation of bias voltage or the variable capacitance of the SMV diodes; these amplitudes are recapitulated in Table 1.

Finally, the transmission coefficient is represented in Figure 6, where the values of the parameters

Table 1. The variation of the S_{ij} amplitudes as a function of the bias voltage.

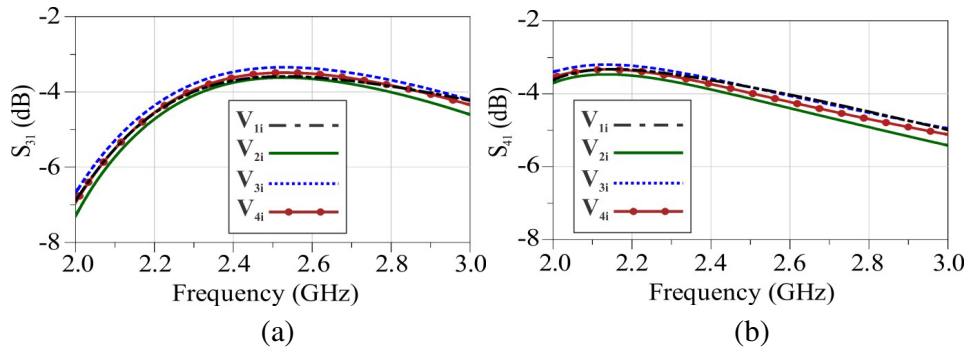|	V_1 (D_1) (V)	V_2 (D_2) (V)	V_3 (D_3) (V)	V_4 (D_4) (V)	V_5 (D_5) (V)	V_6 (D_6) (V)
V_{1i}	10	10	15	20	0	0
V_{2i}	10	10	15	9.5	0	0
V_{3i}	10	10	15	2.4	0	0
V_{4i}	20	0	10	20	7	20

Figure 6. Simulation results of the transmissions coefficients at: (a) S_{31} between P_1 and P_3, (b) S_{41} between P_1 and P_4.

S_{31} and S_{41} around 2,4 GHz are slightly below the value of -3 dB, which proves that the input power in P_1 is evenly divided into two halves, and each half-power is transmitted successively to the ports P_3 and P_4.

To summarize the simulation results obtained above, we can say that the S-parameter of the proposed adjustable phase coupler proves its high performance around the central frequency, especially, in terms of transmission, reflection, and isolation parameters.

4. EXPERIMENTS AND MEASUREMENT RESULTS

The prototype of the adjustable phase coupler was realized on a single-layer substrate with a relative dielectric constant $\varepsilon_r = 4.3$, thickness $H = 0.8$ mm, and tangent loss Tan$D = 0.021$ with six varactor diodes type SMV2019-079L. As illustrated in Figure 7, the structure is symmetric, so the parameters
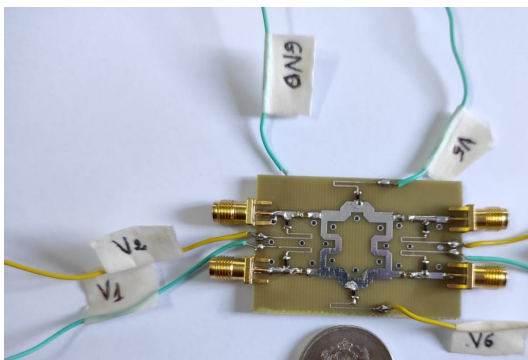

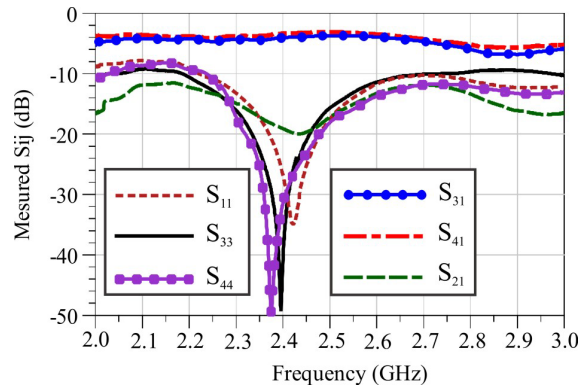**Figure 7.** Photograph of the adjustable phase coupler.

Figure 8. The S-parameters measurement of the adjustable phase coupler.

S_{ij} are independent of the polarization of the device.

The measurements presented below were realized using the Rohde & Schwarz ZVB20 Vector Network Analyzers with an operating frequency range varying from 2 GHz to 3 GHz. The number of points chosen is equal to 2001 to minimize the measurement errors, and the S_{ij} measured are shown in Figure 8, in which we can observe clearly that the module of the S_{ii} parameters is a -35 dB for S_{11}, and it reaches -50 dB for both S_{22} and S_{44}. In this aspect, the measured reflection coefficient too is closely equal to that previously obtained in the simulation results.

The same can be said for the parameter S_{21}, and as it was expected, around the central frequency it decreases to the value -20 dB which means a good isolation between the ports of the coupler.

Throughout the range of frequencies from 2 GHz to 3 GHz, the S_{31} and S_{41} parameters continued to oscillate tightly around -3 dB which is in accordance with the simulation results.

The second part of this work is directed to the study of the phase difference between the two output line signals to conclude on the adequacy of the adjustable phase coupler since the phase difference is an important parameter in the coupler's application, and in this case, it is expressed by:

$$\Delta\varphi = \text{phase}\,(S_{44}) - \text{Phase}(S_{33}) \tag{14}$$

The phase shifts of the ports P3 and P4 from $0°$ to $180°$ by the diodes are arranged in Table 2.

Table 2. Phase shifts of the ports P3 and P4 from $0°$ to $180°$.

$\Delta\varphi$	$0°$	$45°$	$90°$	$120°$	$145°$	$180°$
V_{ii} (V)	V_{i1} (V)	V_{i2} (V)	V_{i3} (V)	V_{i4} (V)	V_{i5} (V)	V_{i6} (V)
V_1 (V)		5	9	10	13	20
V_2 (V)		5	9	10	13	20
V_3 (V)	8	0	0	5	10	17
V_4 (V)	8	0	0	5	10	17
V_5 (V)	20	10	15	0	0	0
V_6 (V)	20	10	15	0	0	0

The phase differences obtained by simulation and measurements are represented in Figures 9(a) and (b); there is a perfect agreement, especially in the frequencies ranging from 2.3 GHz to 2.6 GHz surrounding the central frequency. A small delay in the signals can be noticed, and fortunately, this does not affect the performance of the coupler. This delay is due to the welding and calibration at the time of the realization of the device.

As predicted, the figure shows that the phase differences obtained around 2,4 GHz are exactly equal to 0, $45°$, $90°$, $120°$, and $180°$ corresponding to V_{i1}, V_{i2}, V_{i3}, V_{i4}, V_{i5}, and V_{i6} for both the simulation and measurements results, which is the desired result for the proposed adjustable phase coupler of this wok. In Table 3, we summarize the principal results obtained and compared those to previous works.

Table 3. A comparison between the results of this work and previously published results.

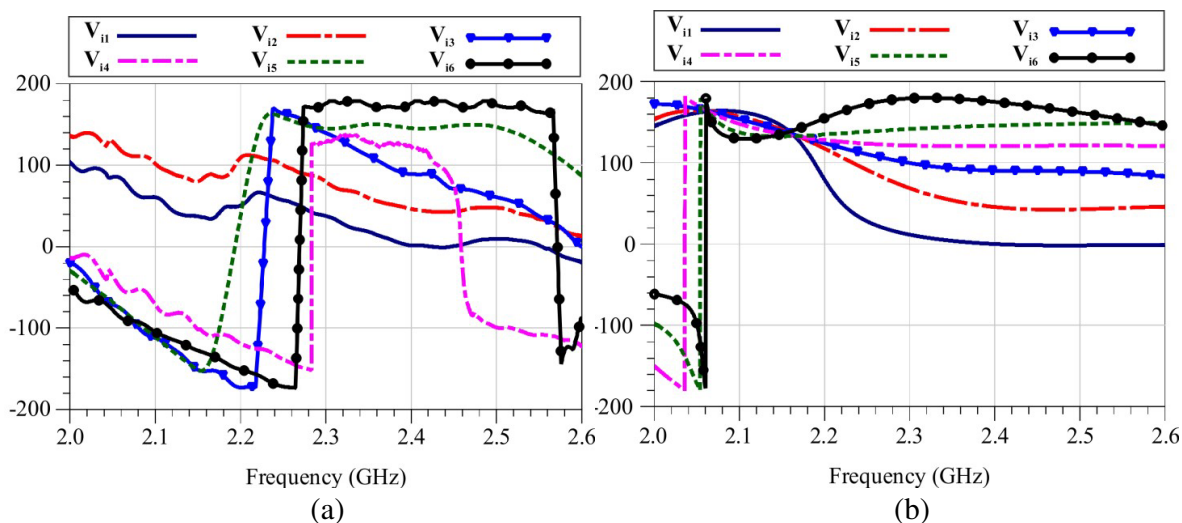|	Ref. [12]	Ref. [13]	[This work]
Central frequency (GHz)	2.2	2.0	2.4
Size in Electrical Length	$0.367\lambda_0 \times 0.143\lambda_0$	$0.433\lambda_0 \times 0.2\lambda_0$	$0.384\lambda_0 \times 0.248\lambda_0$
Reflection coefficient (dB)	-19.671	-18	Better than -30
Isolations coefficient (dB)	-19.542	-25	Better than -27
Transmission coefficient (dB)	$-3.088; -3.229$	3.02	$-3.075; -3.765$
Phase difference	$89.766°$	$\sim 89.225°$	$0°–45°–90°–120°–180°$

Figure 9. Phase difference by: (a) measurements and (b) simulation.

The data presented in the table above relate to the characteristics of the different couplers with an exclusive phase shift from 0° to 180°, because few works deal with all the phases simultaneously as in this work. However, a comparison of the parameters given in this table highlights the proper functioning and performance of this adjustable coupler.

5. CONCLUSION

Overall, the experimental results are consistent with the simulated ones in the considered frequency range of 2.4 GHz. In both cases, the reflection and isolation coefficients were below -27 dB and around -40 dB for the majority of the ports. The transmission coefficient also showed high performance, slightly lower than -3 dB around the center frequency. The phase shifts obtained in the output signals corresponded perfectly to the desired values for the proposed adjustable phase coupler, covering all phases: 0, 45°, 90°, 120°, and 180°. In addition, the coupler has small dimensions, so it can be easily integrated into any circuit. This indicates that the adjustable phase coupler has promising potential in many applications to consider in the future.

REFERENCES

1. Kim, S., S. Yoon, Y. Lee, and H. Shin, "A miniaturized Butler matrix based switched, beamforming antenna system in a two-layer hybrid stackup substrate for 5G applications," *Electronics*, Vol. 8, 1232, 2019, doi: 10.3390/electronics8111232.

2. Han, K., W. Li, and Y. Liu, "Flexible phase difference of 4×4 Butler matrix without phase-shifters and crossovers," *International Journal of Antennas and Propagation*, Vol. 2019, Article ID 4703161, 7 pages, 2019, https://doi.org/10.1155/2019/4703161.

3. Hao, Z. C., W. Hong, J. X. Chen, H. X. Zhou, and K. Wu, "Single-layer substrate integrated waveguide directional couplers," *IEE Proc. Microwave Antennas Propag.*, Vol. 153, No. 5, 426–431, Oct. 2006.

4. Babale, S. A., S. K. Abdul Rahim, O. A. Barro, M. Himdi, and M. Khalily, "Single layered 4×4 Butler matrix without phase-shifters and crossovers," *IEEE Access*, Vol. 6, 77289–77298, 2018.

5. Wang, Y., K. Ma, N. Yan, and L. Li, "Design of broad band SIW couplers with 45° and 90° phase difference," *Proceedings of iWEM 2014*, Sapporo, Japan, 2014.

6. Liu, H., X. Li, Y. Guo, S.-J. Fang, and Z. Wang, "Design of filtering coupled-line trans-directional coupler with broadband bandpass response," *Progress In Electromagnetics Research M*, Vol. 100, 163–173, 2021.

7. Muquaddar, A., K. K. Sharma, and R. P. Yadav, "Design and analysis of a stub-less capacitive loaded branch line coupler with improved bandwidth performance," *Progress In Electromagnetics Research M*, Vol. 95, 105–114, 2020.

8. Liu, H., X. Wang, T. Zhang, S.-J. Fang, and Z. Wang, "Design of full-360° reflection-type phase shifter using trans-directional coupler with multi-resonance loads," *Progress In Electromagnetics Research Letters*, Vol. 101, 63–70, 2021.

9. "Microwave power dividers and couplers tutorial," http://www.markimicrowave.com/menus/appnotes/Microwave_Power_Dividers_and_Couplers_Primer.pdf, Marki Microwave, accessed Jan. 2012.

10. Pozar, D., *Microwave Engineering*, 3rd Edition, Wiley, New York, 2005.

11. https://www.keysight.com/zz/en/home.html, Jan. 2022.

12. Moubadir, M., H. Aziz, N. A. Touhami, and A. Mohamed, "A miniaturized branch-line hybrid coupler microstrip for long term evolution applications," *Procedia Manufacturing*, Vol. 22, 491–497, 2018.

13. Dinh, T. A. N., L. H. Duc, D. B. Gia, and D. Dancila, "A design of wideband high-power 3-dB quadrature coupler using defected ground structure for status data transmitting system," *Bulletin of Electrical Engineering and Informatics*, Vol. 9, No. 1, Feb. 2020.